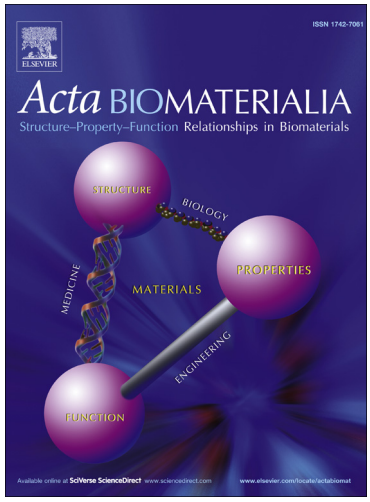

Chitosan-based dressings loaded with neurotensin-an efficient strategy to improve early diabetic wound healing

Liane I.F. Moura, Ana M.A. Dias, Ermelindo C. Leal, Lina Carvalho, Hermínio C. de Sousa, Eugénia Carvalho

PII: S1742-7061(13)00504-7
DOI: http://dx.doi.org/10.1016/j.actbio.2013.09.040
Reference: ACTBIO 2932

To appear in: *Acta Biomaterialia*

Received Date: 11 June 2013
Revised Date: 20 September 2013
Accepted Date: 30 September 2013

Please cite this article as: Moura, L.I.F., Dias, A.M.A., Leal, E.C., Carvalho, L., de Sousa, H.C., Carvalho, E., Chitosan-based dressings loaded with neurotensin-an efficient strategy to improve early diabetic wound healing, *Acta Biomaterialia* (2013), doi: http://dx.doi.org/10.1016/j.actbio.2013.09.040

Chitosan-based dressings loaded with neurotensin-an efficient strategy to improve early diabetic wound healing

Liane I. F. Moura[1,2], Ana M. A. Dias[2], Ermelindo C. Leal[1], Lina Carvalho[3], Hermínio C. de Sousa[2*], Eugénia Carvalho[1,4*]

[1]*Center of Neuroscience and Cell Biology, University of Coimbra, 3004-517 Coimbra, Portugal*
[2]*CIEPQPF, Chemical Engineering Department, FCTUC, University of Coimbra, Rua Sílvio Lima, Pólo II – Pinhal de Marrocos, 3030-790 Coimbra, Portugal*
[3]*Institute of Pathology, Faculty of Medicine, University of Coimbra, 3004-517 Coimbra, Portugal*
[4]*APDP, The Portuguese Diabetes Association, Rua do Salitre, nº. 118-120, 1250-203Lisboa, Portugal*

[*]Corresponding authors:

Eugénia Carvalho
Center for Neurosciences and Cell Biology,
University of Coimbra,
3004-517 Coimbra, Portugal
Phone: +351 239 855 760
Fax: +351 239 853 409
E-mail address: ecarvalh@cnc.uc.pt

Hermínio C. de Sousa
CIEPQPF, Chemical Engineering Department, Faculty of Science and Technology,
University of Coimbra,
3030-790 Coimbra, Portugal
Phone: +351 798 700
Fax: +351 798 703
E-mail address: hsousa@eq.uc.pt

Abstract

One important complication of *diabetes mellitus* is the chronic, non-healing diabetic foot ulcer (DFU). This study aims to develop and use dressings based on chitosan derivatives for the sustained delivery of the neurotensin (NT), a neuropeptide that act as an inflammatory modulator in wound healing. Three different derivatives, namely N-carboxymethyl chitosan (CMC), 5-methyl pyrrolidinone chitosan (MPC) and N-succinyl chitosan (SC), are presented as potential biomaterials for wound healing applications. Our results showed that MPC has the best fluid handling capacities and delivery profile being also non-toxic to Raw 264.7 and HaCaT cells. NT-loaded and non-loaded MPC dressings were applied into control/diabetic wounds to evaluate their *in vitro*/*in vivo* performances and the results show that the first induced a faster healing (50% wound area reduction) in the early phases of wound healing in diabetic mice. NT-loaded MPC foam also reduced inflammatory cytokines expression namely TNF-α ($p<0.001$) and decreased the inflammatory infiltrate at day 3. At day 10, MMP-9 is reduced in diabetic skin ($p<0.001$) increasing significantly fibroblasts migration and collagen (COL1A1, COL1A2 and COL3A1) expression and deposition. These results suggest that MPC-based dressings may work as an effective support for a NT sustained release to modulate DFU.

Keywords: Chitosan derivatives; wound dressings; diabetic foot ulcers; neurotensin; wound healing

Abbreviations:

Collagen type I, alpha 1 (COL1A1)

Collagen type I, alpha 2 (COL1A2)

Collagen type III, alpha 1 (COL3A1)

Diabetic foot ulcer (DFU)

Ditio-bis(nitrobenzoic acid) (DTNB)

Endothelial growth factor (EGF)

Extracellular Matrix (ECM)

Fetal bovine serum (FBS)

Glutathione (GSH)

Interleukin-1β (IL-1β)

Interleukin-6 (IL-6)

Interleukin-8 (KC)

Metalloproteinase 9 (MMP-9)

N-carboxymethylchitosan (CMC)

Neurotensin (NT)

Nitric oxide (NO)

N-succinyl chitosan (SC)

Phosphate buffer solution (PBS)

Platelet-derived growth factor (PDGF)

Polymorphonuclear leukocytes (PMN)

Scanning electron microscopy (SEM)

Streptozotocin (STZ)

Transforming growth factor β1 (TGF β1)

Transforming growth factor β3 (TGF β3)

Tumor Necrosis Factor -α (TNF-α)

Vascular endothelial growth factor (VEGF)

1. Introduction

Diabetes mellitus is one of the most prevalent chronic diseases worldwide. Impaired wound healing is a complication of diabetes that results in the failure to completely heal diabetic foot ulcers (DFUs) [1]. Complications of DFUs lead to frequent hospitalizations and in extreme cases, to amputations that result in elevated hospital costs and poor quality of life for patients [2]. DFU is a multifactorial complication that results particularly as a consequence of peripheral neuropathy, impaired vascular function, impaired angiogenesis and/or chronic inflammation [1, 3].

Recently, it became evident that peripheral nerves and cutaneous neurobiology contributes to wound healing [4]. Loss of peripheral sensory and autonomic nerves reduces the production of neuropeptides that are important for proper wound healing [3]. Neurotensin (NT) is a bioactive neuropeptide that is widely distributed in the brain and in several peripheral tissues [5, 6]. NT interacts with leukocytes, mast cells, dendritic cells and macrophages leading to cytokine release and chemotaxis that can modulate the immune response. In addition, NT affects microvascular tone, vessel permeability, vasodilation/vasoconstriction and new vessel formation which helps to improve angiogenesis during wound healing processes [3, 7, 8].

Some studies demonstrated that topical application of neuropeptides, such as substance P and neuropeptide Y can improve wound healing in diabetes [9, 10]. However, the major problem of topical administration of peptides is their short half-life and loss of bioactivity in the peptidase-rich wound environment [11]. An alternative strategy to overcome this problem is the use of biocompatible wound dressings for the sustained delivery of neuropeptides. These dressings should however also replicate skin characteristics in order to promote the proliferation and migration of fibroblasts and keratinocytes, as well as to enhance collagen synthesis, leading to proper healing with low scar formation [12, 13].

Wound dressings based on natural polymers have been extensively applied to simulate extracellular matrix (ECM) regeneration after injury [12, 13]. One of the most used natural-based polymer for wound healing applications is chitosan [12], which is a linear copolymer of D-glucosamine and *N*-acetyl-D-glucosamine [14]. Since it is derived from chitin, a polymer found in fungal cell walls and crustacean exoskeletons, it is a relatively inexpensive and abundant material [15]. In addition, it has proven to be biodegradable, biocompatible, non-antigenic, non-toxic, bioadhesive, anti-microbial,

bioactive and to have haemostatic capacity [15-17]. Furthermore, chitosan promotes tissue granulation and accelerates wound healing through the recruitment of inflammatory cells such as polymorphonuclear leukocytes (PMN) and macrophages to the wound site [18].

To increase its poor solubility in water, chitosan functional groups can be chemically modified to originate water soluble chitosan derivatives such as *N*-carboxymethyl chitosan (CMC), 5-methyl pyrrolidinone chitosan (MPC) and *N*-succinyl chitosan (SC) [19-21]. These chitosan derivatives are functional biomaterials that maintain the antibacterial and non-cytotoxic properties of parent chitosan. In addition, they stimulate extracellular lysozyme activity of skin fibroblasts [22, 23].

The aim of this study was to develop and apply wound dressings, prepared from the chitosan derivatives referred above (CMC, MPC, SC), for a prolonged and efficient NT delivery into diabetic and non-diabetic wounds, and also confer wound protection and comfort. The progression of skin wound healing in diabetic and non-diabetic mice was also evaluated by the analysis of the inflammatory and angiogenic effects of NT when applied in skin wounds alone or loaded into MPC-based dressings.

2. Materials and methods

2.1 Materials

Chitosan (medium molecular weight, degree of acetylation of 90% confirmed by ^{1}H-NMR), glyoxylic acid monohydrate (98%), sodium hydroxide, sodium borohydride (99.5%), levulinic acid (98%), succinic anhydride (97%), reduced GSH, DTNB, dialysis membranes (Spectra/Por (6)) with a MWCO of 8000 Da and methanol p.a., were obtained from Sigma-Aldrich (USA). Acetic acid was obtained from Panreac (Spain), and ethanol was purchased from Riedel-de-Haen (Germany). Ketamine (Clorketam 1000) was obtained from Vétoquinol (Portugal) and xylazine (Rompun) from Bayer HealthCare (Germany). NT was purchased from Bachem (Switzerland). The antibodies against TNF-α and MMP-9 were purchased from Cell Signaling Technology (USA) and the antibodies against VEGF and actin were purchased from the Millipore Corporation (USA).

178 **2.2 Synthesis of chitosan derivatives CMC, MPC, SC**

179 Chitosan (2 g) reacted with glyoxylic acid (1,16 g), levulinic acid (5ml) or succinic
180 anhydride (3 g) to synthesize CMC, MPC and SC respectively [24, 25], following by
181 precipitation with ethanol and dialysis to remove unreacted reagents. Foams of CMC,
182 MPC and SC were prepared by freeze-drying adding 1.5 ml of each solution in 12 multi
183 well plates. The average thickness of the obtained materials was 250±15 µm. All
184 samples were stored at −20 °C, away from light and humidity before usage. The degree
185 of substitution of each of the derivatives was calculated by ^{1}H-NMR using a Bruker
186 Avance III 400 MHz spectrometer, with a 5-mm TIX triple resonance detection probe
187 using D_2O acidified with acetic acid (10 µl of acetic acid in 600 µl of D_2O).
188
189 **2.3 Scanning electron microscopy (SEM)**
190 SEM micrographs were obtained at 5 kV (Jeol, model JSM-5310, Japan). Samples were
191 coated with gold (approximately 300 Å) in an argon atmosphere.
192
193 **2.4 Water vapor and water sorption capacities**
194 Samples of CMC, MPC and SC, with 22 mm of diameter, were dried at 37 °C for 72 h
195 until constant weight was achieved. Both water vapor and water sorption capacities
196 were measured gravimetrically. In the first case, dried foams were exposed to a 95%
197 relative humidity atmosphere, in a desiccator containing a saturated solution of
198 potassium sulfate at 32 °C accordingly to Dias et al, 2013 [26]. In the second case,
199 samples were immersed into phosphate buffer (pH 7) at 37 °C and weighted after
200 removing the surface phosphate buffer using filter paper.
201 Samples were weighted at fixed time intervals until they reach equilibrium. The water
202 vapor and water sorption capacities were calculated as the ratio between sample weight
203 at time *t* and sample initial dry weight. All the samples were measured in duplicate.
204
205 **2.5 *In vitro* release kinetics**
206 Kinetic release profiles of GSH were performed spectrophotometically (Jasco, model
207 630, Japan) at 412nm. Known amounts of a GSH solution (5 mM) were loaded into
208 previously weighted samples of each polymer. The GSH solution has been previously
209 placed in an ultrasonic bath to avoid oxidation. After drying, samples were immersed in
210 phosphate buffer at pH 6, 7 or 8 at 32 ºC, under orbital stirring (100 rpm) during 8 h.

The quantification of released GSH was based on the Ellman's Test. This test is based on the addition of 5,5'-dithio-*bis*-(2-nitrobenzoic acid) (DTNB), a yellow water-soluble compound, that reacts with free sulfhydryl groups in peptide solution. At pre-determined time periods, an aliquot (100 µl) of the released solution was removed and analyzed with a mixture of 1800 µL of phosphate buffer and 100 µl of DNTB stock solution (20 mM). Fresh 100 µL of phosphate buffer was added each time point to the medium. Each sample was analyzed in duplicate.

2.6 Cell culture

Mouse leukaemic monocyte macrophages (Raw 264.7) and human keratinocyte (HaCaT) cells were cultured in DMEM medium, pH 7.4, supplemented with 10 % heat inactivated fetal bovine serum (FBS), 3.02 g/l sodium bicarbonate, 30 mM glucose, 100 U/ml penicillin, 100 µg/ml streptomycin, at 37 ºC in a humidified incubator containing 5% CO_2. Sub-culturing was performed according to ATCC recommendations. Raw 264.7 and HaCaT cell lines were purchased by ATCC (number TIB-71) and CLS (number 300493), respectively.

2.7 MTT assay

Raw 264.7 (8×10^4 cells/well) and HaCaT (4×10^4 cells/well) cells were plated individually in 12-well plates with 430 µL of DMEM, above the previously sterilized biomaterials (UV light for at least 30 minutes). After 24 and 48 h of incubation, 43 µl of 3-(4,5-dimethylthiazol-2-yl)-2,5-diphenyltetrazolium bromide (MTT) solution (5mg/ml) was added to each well. The plates were further incubated at 37 ºC for 1 h, in a humidified incubator containing 5% CO_2. After this period, 300 µl of acidic isopropanol (0.04 N HCl in isopropanol) was added. Quantification was performed using an ELISA automatic microplate reader (SLT, Austria) at 570 nm, with a reference wavelength of 620 nm. Each sample was analyzed in duplicate.

2.8 NO production – Griess Method

Raw 264.7 (8×10^4 cells/well) cells were plated in 12-well plates with 430µL of DMEM, above the previously sterilized biomaterials (UV light for at least 30 minutes). After 24 and 48 h after incubation, 170 µl of medium supernatant was mixed with an equal volume of Griess reagent (1% sulfanilamide, 0.1% N-1-naphthelenediamine

dihydrochloride in 2.5% phosphoric acid). After 30 minutes of incubation in the dark, the absorbance was measured at 550 nm in a microplate reader (SLT, Austria). Nitrite concentration was calculated from a previously obtained nitrite standard curve.

2.9 *In vivo* wound closure

We used male C57BL/6 mice (Charles River Corporation Inc, Barcelona, Spain) weighing 25-30 g. The animals were maintained at normal room temperature (22-24 °C) on a 12 h light/dark cycle, with free access to commercial pellet diet and water. After the wound procedure, the animals were kept in individual cages. All experiments were conducted according to the National and European Communities Council directives on animal care.

Diabetes was induced by a single intraperitoneal injection of streptozotocin (STZ, 150 mg/kg) in citrate buffer pH 4.5. Four days after diabetes induction, blood glucose levels were checked by Accu-Chek Aviva glucometer (Roche Diagnostics GmbH, Germany). The animals with blood glucose levels higher than 300 mg/dl were considered diabetic. Mice were anesthetized by intraperitoneal injection of xylazine (13 mg/kg) and ketamine (66.7 mg/kg). The dorsal hair of control and diabetic mice was shaved and two 6 mm diameter full-thickness wounds of were created with a biopsy punch.

C57BL/6 mice were randomly divided into six groups of treatment for control (non-diabetic) and diabetic mice – three groups for day 3 (d3) (I, II, III) and three similar groups for day 10 (d10) (IV, V, VI): groups I and IV were treated with MPC dressings alone (6-12 animals), groups II and V with topical application of 50 µg/ml NT (7 animals) and groups III and VI with 50 µg/ml NT-loaded MPC dressings (7-9 animals).

For each animal one of the wounds worked as control (PBS application only) and the other received treatment. The dried MPC foams were applied over the wounds and wetted with 5 µl of PBS or NT solution (50 µg/ml) to originate hydrogels with improved adherence and mucoadhesive capacities. By visual inspection it was possible to observe that the dressings persist into the wound approximately until day 6-7. The progress of wound healing was evaluated periodically by acetate tracing till day 10. Topical application of PBS or NT (alone or loaded into the prepared MPC dressing) was performed daily. At day 3 or day 10, C57BL/6 mice were sacrificed and around 2 mm of tissue and skin surrounding the wound were harvested. These time points were

chosen to evaluate the inflammatory (day 3) and the proliferating/remodeling (d10) phases of wound healing.

2.10 Real time RT-PCR

Total RNA was isolated from skin with the RNeasy Mini Kit according to the manufacturer's instructions (Qiagen, USA). First strand cDNA was synthesized using High Capacity cDNA Reverse Transcription. Then, real-time RT-PCR was performed in a BioRad MyCycler iQ5. Primer sequences are given upon request. Gene expression changes were analyzed using iQ5Optical system software v2. The results were normalized using a housekeeping gene, TATA box binding protein (TBP), which was previously validated in our lab. Quantitative RT-PCR results were analyzed through delta CT calculations.

2.11 Western Blotting

Skin tissue lysate was homogenized in RIPA buffer (50mM Tris HCl pH8, 150 mM NaCl, 1% NP-40, 0.5% Sodium Deoxycholate, 0.1% SDS, 2 mM EDTA, proteases inhibitor cocktail, phosphatase inhibitor cocktail and 1 mM DTT). Protein concentration was determined using the BSA method and the skin lysates were denatured at 95 ºC, for 5 min, in sample buffer. 40 µg of total protein were resolved on 12% SDS-PAGE and transferred to PVDF membranes. The membranes were blocked with 5% fat-free dry milk in Tris-buffered saline containing 0.1% (v/v) Tween 20 (TBS-T), for 1 h, at room temperature. After blocking, membranes were incubated with the primary antibodies against the TNF-α (1:500), VEGF (1:1000), MMP-9 (1:500), overnight at 4 ºC. After incubation, membranes were washed and incubated for 1 h at room temperature, with anti-rabbit antibody (1:5000), or anti-mouse antibody (1:5000). The membranes were exposed to the ECF reagent followed by scanning on the VersaDoc (Bio-Rad Laboratories, Portugal). For normalization, the membranes were re-probed with an anti-actin antibody (1:10000). The generated signals were analyzed using the Image-Quant TL software.

2.12 Hydroxyproline content

This analysis was performed using a Hydroxyproline Assay Kit (Sigma Aldrich, USA). Briefly, 10 mg of skin tissue were homogenized in 100 µl of water and hydrolyzed with

HCl 12 M at 120 ºC for 3 h. 25 µl of the supernatant were transferred to 96- well plate and evaporated in the incubator at 60 ºC till total dryness. After, 100 µL of the Chloramine T/Oxidation Buffer and 100 µL of the Diluted DMAB Reagent were added to each sample and incubated for 90 minutes at 60 ºC. Quantification was performed using an ELISA automatic microplate reader (SLT, Austria) at 560 nm.

2.13 Histopathological analysis

For histological preparation, the skin was fixed in 10% neutral buffered formalin and then embedded in paraffin. Skin tissues were sectioned in 3 µm thickness slices for histopathological examination by hematoxylin/eosin (H&E) and for collagen formation by Masson's Trichrome staining, using standard procedures. The stained sections were observed with a microscope Nikon H600L with Digital Camera DXM 1200F (Nikon, Germany). Analysis of stained skin sections was performed by an experienced pathologist.

2.14 Statistical analysis

Results are expressed as mean ± SEM (Structural Equation Modeling). Statistical analysis was performed using one-way ANOVA followed by Tukey's multiple comparison tests or through the unpaired or paired t test by GraphPad Prism (GraphPad Software, Inc., San Diego, CA, USA) and p values lower than 0.05 were considered statistically significant.

3. Results

3.1 Degree of substitution and morphology of CMC, MPC and SC

The degree of substitution (amount of native chitosan amino groups substituted) of each chitosan derivative was confirmed by ^{1}H-NMR and it was equal to 25.5%, 24% and 28.5% for CMC, MPC and SC, respectively (Figure S1 supplementary data). The schematic representation of each derivative is shown in Figure 1A.

The different morphologies obtained for each of the prepared chitosan derivative foams are shown in Figure 1B. CMC presents a honeycomb-like porous structure, with larger pores than MPC and SC, which presented an interlaced fiber-like pattern. The fiber-like structure of SC seems to be thinner than the one observed for MPC.

3.2 Water vapor and water swelling properties

Figure 2A shows the water vapor sorption behavior of CMC, MPC and SC foams in controlled humidity (95%) and temperature conditions (32 ºC). Data show that the hydrophilicity of the materials changes in the sequence SC > MPC > CMC. All the samples achieved equilibrium after approximately 8 hours and at this point, SC adsorbed 35% of its weight in water vapor while MPC and CMC adsorbed 24% and 14%, respectively.

In terms of water swelling capacity, Figure 2B shows that SC presents the fastest swelling rate, reaching its maximum (2438%) after 5 h and it starts to dissolve after this period. On the other hand, CMC presented the lowest swelling capacity (163%) while MPC has an intermediate water swelling profile. Both MPC and SC foams reach water swelling equilibrium after approximately 6 h and both maintain their structure (macroscopically, at naked eye) until day 15, at the tested experimental conditions.

3.3 *In vitro* release kinetics

Glutathione (GSH) was used as a model peptide test molecule for *in vitro* release kinetics studies. The release of GSH from CMC, MPC and SC foams was followed for a period of 8 h at 3 different pHs (6, 7 and 8) which is the pH range that can be observed during the wound healing process. The release profiles measured for each chitosan derivative at pH 7 are presented in Figure 3. Data measured at pHs 6 and 8 are presented as supplementary data (Figure S2) due to the similarities observed among the different pHs studied in this work. The release profiles show that equilibrium is attained between 5 and 8 h for all the samples and that the amount of GSH released from SC is significantly higher than for CMC and MPC (~9 and 4 times higher, respectively). When comparing the amount of GSH released after 8 h with the total GSH loaded amount, the results show that ~50% was released from CMC and MPC while almost 100% was released from SC. Obtained results also show that the amount of GSH released from the chitosan derivatives is not significantly affected in the pH range studied and considering the experimental error, being average equal to (32.33±0.72), (67.65±6.77) and (287.18±14.92) GSH released (%)/$m_{polymer}$ (g) for CMC, MPC and SC, respectively.

3.4 *In vitro* biocompatibility of CMC and MPC

There was no significant difference in the viability of the Raw and HaCaT cells exposed to CMC and MPC foams during 24, 48 and 72 h, when compared to control, as shown in Figure 4 (A and B, respectively). NO is produced by macrophages in response to an inflammatory stimuli. The production of nitrites, final stable breakdown product of NO, measured after exposure of the cells to the chitosan derivatives (Figure 4C) was also not significantly affected, however, a slight increase in the nitrites produced after 72 h was observed, which may be due to the stress to which cells are subjected after this exposure period.

3.5 Wound healing experiments – *in vivo*

Figure 5 shows the effect of the different topical treatments studied in this work: NT alone, MPC foam alone and NT-loaded MPC foam both in control (A) and diabetic (B) mice. PBS was applied as control. All treatments were shown to reduce significantly the wound area, as compared to PBS treated wounds, in both control and diabetic mice. In Figure 5 A, NT alone reduced significantly the wound size at day 3 post wounding, by 22% ($p<0.05$), compared to the PBS treated wounds, in control mice. In diabetic mice, the wound size of the NT treated wounds is also significantly reduced at day 3, and at day 5 by 29% ($p<0.01$) and 34% ($p<0.01$), respectively. A different healing profile is observed for the non-loaded and NT-loaded MPC treated wounds either in control and diabetic mice. A significant decrease in the wound area is evident at day 1 post wounding in non-loaded MPC by 48% ($p<0.001$) and in NT-loaded MPC, by 43% ($p<0.001$), when compared with PBS-treated wounds (Figure 5A). In diabetic animals, the profile of wound closure was similar, however the NT-loaded MPC treatment was significantly more effective than MPC alone, with a wound reduction of 50% ($p<0.001$) instead of 35% ($p<0.001$) of closure for the non-loaded dressing (Figure 5B).

3.6 Cytokine, MMP-9, collagen types and growth factors expression at the wound site

In order to address the pattern of cytokine gene expression in untreated or treated wounds at 0, 3 and 10 days post-wounding, the gene expression for inflammatory cytokines (TNF-α, IL-6, KC, IL-1β) and several types of collagen genes (COL1A1, COL1A2, COL3A1) were measured and the results are presented in Figure 6 A-N. Other important factors such as MMP-9, growth factors (EGF, VEGF, PDGF), TGFβ1,

TGFβ3 were also evaluated and its expressions are presented in Figure S3 Supplementary data.

In unwounded skin (day 0, baseline), all the measured inflammatory cytokines were significantly increased in the skin of diabetic animals compared with the healthy controls (Figure 6 A-G). On the other hand, all types of collagens analyzed are significantly reduced ($p<0.001$) (Figure 6 I-N, respectively).

We observed a significant increase, at day 3 post-wounding, in the inflammatory stimulus, as one might expect, when compared to day 0 in controls. However, the same effect is not observed in diabetic mice.

Furthermore, at day 3, in control mice, the MPC treatment alone reduced significantly the expression of TNF-α ($p<0.05$), IL-6 ($p<0.05$) and IL-1β ($p<0.05$) while the NT alone decreased the expression of TNF-α ($p<0.05$) and IL-1β ($p<0.05$) (Figure 6 A, C and G, respectively). In addition, the NT-loaded MPC treatment reduced the TNF-α expression ($p<0.05$), however the IL-6 and KC expression significantly increased in the controls ($p<0.05$). In diabetic mice, the TNF-α expression was significantly higher for all treatments ($p<0.05$) but the IL-1β expression is reduced upon the NT-loaded MPC treatment ($p<0.05$) compared with PBS alone.

Moreover, at day 3, NT alone reduced the EGF expression in diabetic mice ($p<0.05$) and increased the VEGF expression ($p<0.05$) in the control (Figure S3 C and E). In addition, while NT and NT-loaded MPC foam significantly induced TGFβ3 expression ($p<0.001$), in controls, no differences where observed in diabetic skin (Figure S3 K). Collagen genes were more expressed in control skin and NT treatment significantly increased COL1A1, COL1A2 and COL3A1 expression in diabetic skin (Figure 6 I, K and M, respectively).

At day 10, the expression of all the inflammatory cytokines was diminished to baseline levels in the controls, with the exception of TNF-α that increase ($p<0.05$) with NT and the NT-loaded MPC application, compared to PBS treated wounds. In diabetic mice, all the treatments reduced the expression of TNF-α, IL-6 and KC ($p<0.05$ in all cases) (Figure 6 B, D and F, respectively). The non-loaded and the NT-loaded MPC treatments caused a decrease in the MMP-9 expression in both control and diabetic mice ($p<0.05$) (Figure S3 B). In addition, the NT-loaded MPC treatment reduced EGF in diabetic mouse skin ($p<0.05$) (Figure S3 D).

NT and NT-loaded MPC foam significantly induced TGFβ1 and TGFβ3 expression ($p<0.001$) in controls at day 10 but no differences where observed in diabetic skin. In diabetic skin, only NT treatment reduced significantly TGFβ3 ($p<0.05$) (Figure S3 J, L). In addition, NT and NT-loaded MPC foam highly stimulated an increase in COL1A1 and COL1A2 ($p<0.001$) in control mice while in diabetic mice only NT-loaded MPC significantly induced expression of all collagen genes (Figure 6 J, L,N).

3.7 Protein expression in the wound site

To evaluate protein expression levels at the wound site, Western Blot analysis of skin tissue was performed (Figure 7). At day 0, only MMP-9 is significantly increased ($p<0.001$) in diabetic mice when compared to controls. At day 3, NT treatment induced a reduction of MMP-9 protein levels in control mice. Moreover, in diabetic wounds, MPC treatment increased TNF-α level. In contrast, NT and NT-loaded MPC foam significantly reduced MMP-9 ($p<0.05$) and TNF-α ($p<0.001$) protein levels, respectively.

At day 10, MPC, NT or NT-loaded MPC treatments significantly reduced MMP-9 protein expression comparing with PBS treatment, either in control or diabetic skin. In addition, TNF-α protein expression was not detected in all treatments at day 10, by Western Blot.

3.8 Hydroxyproline content in the wound site

To evaluate collagen deposition in mouse skin, hydroxyproline levels were measured in unwounded and wounded (treated and non-treated) skin (Figure 8). In unwounded skin, hydroxyproline levels were significantly decreased ($p<0.01$) in diabetic mice comparing with control skin. At day 3 post-wounding, NT significantly increased ($p<0.05$) hydroxyproline content in diabetic skin, while at day 10, this effect was observed with NT-loaded MPC in control and diabetic skin ($p<0.05$, $p<0.01$), respectively.

3.9 Histopathological analysis of the wound

For the histopathological analysis of control and diabetic skin tissue we used the H&E and Masson´s Trichrome staining (Figures 9A and B, respectively). In unwounded skin the increase in the epidermis skin thickness was evident in diabetic mice when compared with control. At day 3 post wounding, all the treatments stimulated an

increase in the epidermis thickness which was more significant for the non-loaded and NT-loaded MPC treatments in diabetic skin (Table 1). At day 10, the epidermis thickness profile was similar with a stronger effect in diabetic skin (Figure 9A – 3), (Table 2). A specific re-epithelialization profile was observed: in control mice, re-epithelialization occurred from bottom to top with basal cells in the epidermis covering the scar. In diabetic mice, the re-epithelialization occurred over the granulation inflammatory tissue while this was suffering repair, without correlation with the applied treatments, in both groups (Table 2 and 3).

At day 3, neither MPC, NT alone or NT-loaded MPC treatments affected the number of polymorphonuclear leukocytes (PMN) and lymphocytes in control skin, however in diabetic skin, these inflammatory cells were less recruited to the wound site compared with the PBS treatment. In addition, there is higher production of fibrin in diabetic skin while no plasma cells were observed in either control or diabetic skin (Table 3). At day 10, there was no significant recruitment of PMN and lymphocytes observed in control skin, while in diabetic wounds treated with either MPC, NT alone or NT-loaded MPC, PMN cells, lymphocytes and plasma cells were present in higher numbers when compared with PBS treatment. It is important to note that inflammatory cells persisted at day 10 especially in the diabetic wounded skin. No fibrin was observed either in control or diabetic skin (Table 4). Fibroblasts, which are important for tissue repair, were increased in diabetic when compared to control wounded skin, at day 3. Moreover, collagen matrix production appeared to be more evident in diabetic skin, particularly after the NT or the NT-loaded MPC foam treatment. However, the scar was more pronounced in these treatments (Table 3). Furthermore, at day 10, NT-loaded MPC foam induced the migration of fibroblasts and the production of the collagen matrix. However, the scar obtained after this treatment was more pronounced (Table 4). A summary of cytokine expression and corresponding cell type production, in wounded control and diabetic skin, at either day 3 or 10 post-wounding, is represented on table 5.

4. Discussion

One of the main objectives of this work was to evaluate the capacity of chitosan-based wound dressings to work as biocompatible and biodegradable supports for the sustained delivery of neurotensin (NT), a neuropeptide that has shown to improve wound healing [27, 28].

Three different water soluble chitosan derivatives (CMC, MPC and SC) were synthesized and tested for their water swelling capacities and peptide release profiles in order to infer which of the derivatives would present the best performance (controlled swelling and NT delivery over time) *in vivo*. At this stage, GSH was used as a model peptide. Although GSH presents lower molecular weight than NT, it has similar functional groups that will permit the simulation of the physical and chemical interactions that may be established between the molecule and the material used as the dressing.

The obtained results showed that the SC foam has the highest water vapor and water swelling capacity probably due to the high number of thin fibers that constitute its matrix, increasing the contact area between the material and the water molecules. The higher affinity of SC for water (higher hydrophilicity) justifies its faster dissolution in PBS. These results are also in agreement with the ^{1}H-NMR data that showed a higher degree of substitution for SC. This was expected since chitosan substitutions performed in this work aimed to improve the solubility of chitosan in aqueous media. According to the water swelling results, MPC presented an intermediate swelling profile, despite the apparent larger porosity of the CMC derivative observed by SEM analysis.

Medicated wound dressings have been largely used to deliver healing enhancers and therapeutic substances, such as growth factors or stem cells to stimulate wound healing [29, 30]. Their use allows the protection of the wound against external aggression and avoids the rapid biodegradation of the bioactive healing enhancers that may occur in the enzyme rich wound environment. In this work, the capacity of each dressing to sustain the release of a peptide at different pH conditions was addressed. The measured release kinetics performed was not significantly affected within the pH ranges studied and SC is the material that presented the faster release of GSH, followed by MPC and CMC. The release profiles are in accordance with the water swelling profiles observed for the different chitosan derivatives, indicating that the GSH release is mainly controlled by the water swelling capacity of the material and therefore GSH is released mainly through a diffusion mechanism. The higher swelling capacity of SC leads to a higher amount of water inside the polymer structure, better dissolving GSH, enhancing its release into the surrounding medium. According to these results (water swelling and GSH release data), and considering that sustained profiles were envisaged for *in vivo* applications, the use of SC based material was discarded at this stage.

The biocompatibility of CMC and MPC foams was tested *in vitro*, in Raw 264.7 and HaCaT cell lines and the results showed that both materials were non-toxic against these cell lines, up to 48 h. For the 72 h test period, a slight decrease (not statistically significant) in the viability of the cells was observed probably due to foam dissolution or cell stress in the media conditions. Similar results were observed in L929 cells (fibroblast cell line) by Huang and colleagues [31]. The production of nitrites by macrophages Raw 264.7 was also quantified since it is known that these cells produce NO when stimulated by inflammatory stimulus. The results presented show that CMC and MPC do not increase nitrite levels *in vitro* suggesting that these compounds do not induce an inflammatory response which is in accordance with data previously reported in the literature [32]. The *in vitro* results indicate that both CMC and MPC could be used for wound dressing applications. However, in this work, *in vivo* application and characterization was performed only for MPC, which was the material that presented an intermediate GSH release profile compared to either CMC or SC.

Several studies suggested that chitosan and derivatives accelerate wound healing [33, 34]. For instance, MPC freeze-dried foams were shown to jellify in contact with biological fluids, being progressively absorbed via enzymatic hydrolysis, promoting regeneration of connective tissues [35]. However, no further studies were found in the literature reporting the effect of MPC alone or in combination with NT in diabetic wound healing.

Diabetes mellitus cause important complications, namely at skin level. The healing process involves several overlapping phases: homeostasis/coagulation, inflammation, proliferation (granulation tissue formation), re-epithelialization and remodeling [36]. All these processes require the interaction of skin cells, cytokines and growth factors released from inflammatory cells, fibroblasts, keratinocytes and epithelial cells [2].

Due to the fact that mouse skin is elastic and has lack of a strong adherence to the underlying structures, wound contraction is usually more rapid than epithelialization which causes a decrease in the overall healing time of mice wounds [37]. Wound closure results show that NT induced a faster closure in diabetic mice, even when applied directly over the wound and compared with control mice. This was expected since it has been reported that topical application of neuropeptides, such as Substance P, stimulate diabetic wound healing [9]. In addition, previous studies in our group observed that NT modulates inflammatory responses in a skin dendritic cell line [28].

Treatments with non-loaded and NT-loaded MPC foams induced a significant reduction of the wound area, especially in the first 3 days post-wounding and in both control and diabetic mice. Moreover, NT-loaded MPC presented a faster healing profile in diabetic skin wounds. These results suggest a synergistic behavior between the bioactivity of NT alone and the intrinsic healing properties of MPC. Moreover and as intended, a sustained release of NT may also occur which guarantees controlled NT levels during the healing process. The adhesive properties of chitosan and its derivatives could explain this enhanced healing profile [38]. In addition, wound contraction is necessary for the healing process, probably due to the enhanced proliferation of fibroblasts due to arising contractile myofibroblasts [39]. Wound contraction is a biologically important process in wound healing, especially in the healing of chronic wounds such as DFU, although excessive contraction may lead to scar formation [40]. All treatments lead to healing however, larger scars were developed over diabetic wounds that were treated with MPC foams, most probably due to the fast initial wound contraction verified in this case.

In unwounded diabetic skin, an overexpression of inflammatory cytokines, growth factors and MMP-9 was observed, which is in agreement with the literature [41]. These results suggest a chronic pro-inflammatory state in diabetic skin that can compromise the wound healing. On the other hand, the gene expression of the different types of collagen is down regulated in the diabetic skin suggesting a decreased capacity of the diabetic skin to produce the appropriate matrix essential for wound healing and skin repair. As decreased expression of COL1A1, COL1A2 and COL3A1 is verified, less collagen is deposited as observed by the hydroxyproline assay [42].

In chronic diabetes, the healing process becomes stalled in one or more of the healing phases originating chronic non-healing wounds. One important phase that can become stalled in diabetes is the inflammatory phase [1]. TNF-α, IL-6, KC and IL-1β are inflammatory cytokines involved in the recruitment of cells, such as neutrophils and macrophages to the wound site, to stimulate the immune response. In the skin, TNF-α produced by inflammatory cells and fibroblasts stimulates adhesion molecules and chemokines leading to attachment of inflammatory cells to vessels, rolling, migration, and eventually chemotaxis into the skin [43]. Moreover, IL-6 and IL-1β, produced by macrophages, fibroblasts, keratinocytes and epithelial cells are also important players in the early phase of inflammation and in the wound healing process [44]. In control mice,

the reduction of TNF-α and IL-1β expression with all treatments, at day 3, suggests a decrease in the inflammatory condition which facilitates healing. In diabetic mice treated with MPC, NT or NT-loaded MPC, less infiltrated inflammatory cells was observed at day 3 comparing with control mice, while TNF-α expression is significantly higher, especially for the MPC alone. Moreover, IL-6 and KC expression is significantly reduced. These results may suggest that high expression of TNF-α is produced not only by inflammatory cells present at the wound site, but also by other cells present at day 3, which can stimulate contraction of the wound and consequently have a beneficial effect in the early stages of wound healing. This may further indicate that in diabetic mice, treated with NT or/and MPC, the granulation tissue fills the wound bed potentiated by the proliferation of skin fibroblasts, in the early phase of wound healing.

Similar results were observed when using MPC alone as treatment. However, NT-loaded MPC treatment induced a decrease in the TNF-α protein content suggesting that the combination of NT with the MPC foam has an effective anti-inflammatory role in wound healing.

At day 10, the inflammatory status persisted in diabetic mice while in controls it is resolved, as expected [4]. On the other hand, all treatments lead to a reduction in the inflammatory cytokines expression supported by the loose conjunctive tissue observed from the beginning, undergoing different status of collagen deposition in diabetic and control mice. At this time point, fibroblasts have an important role in collagen synthesis and scar formation [45, 46]. During the re-epithelialization phase, the initial ECM is gradually replaced by a collagenous matrix with the formation of new blood vessels [47]. The expression of angiogenic factors, VEGF and PDGF, did not change with treatments in diabetic mice possibly showing that these treatments do not stimulate the production of growth factors to improve wound healing.

Our results show that the production of the collagen matrix was higher for MPC and NT-loaded MPC treated diabetic skin, which is correlated with increased scar formation. Obara and colleagues [29] also observed that application of a chitosan hydrogel in diabetic wounds increased scar formation. Moreover, MMP-9 expression in diabetic skin wound was increased at day 3. Most importantly, at day 10, it is observed a decrease of MMP-9 in NT-loaded MPC treated diabetic wounds, while no significant effect is observed in control wounds. Possibly, MMP-9 may affect ECM proteolytic

enzymes, allowing the migration of cells into the wound site, which results in the deposition of new ECM and the development of new tissue. However, it is known that the increased presence of TNF-α in diabetes could reduce the MMP-9/TIMP-2 balance production by fibroblasts, contributing to the elevated proteolytic activity impairing wound healing [48].

As expected, and in agreement with the literature [49], type 1 collagen was the most expressed form of collagen in the skin, serving as the framework for connective tissues such as skin, bone and tendons. This result also agrees with the observed increase in the expression of TGF (Figure S3 supplementary data) which has an important role in the pathophysiology of tissue repair by the enhancement of type 1 collagen gene expression [50].

In addition, at day 3, we observed an increased expression of all types of analyzed collagen in control compared to diabetic skin at the same time point and the opposite is verified at day 10 suggesting that diabetes impair collagen gene expression and deposition in the skin [51]. Moreover, the NT-loaded MPC foam stimulated COL1A1, COL1A2 and COL3A1 expression at day 10 in diabetic skin, which is also correlated with higher collagen production observed by the hydroxyproline content and the Masson´s Trichrome staining.

5. Conclusions

The results obtained in this work show that, in control animals, both MPC and NT-loaded MPC foams have great impact on the early phases of the healing process decreasing the inflammatory infiltrate. In diabetic animals, the major healing effects were observed with either NT alone or NT-loaded MPC foams thus confirming the potential healing effect of NT in diabetic wound. These treatments reduced the inflammatory status in the early phase of wound healing and increased migration of fibroblast and collagen expression and deposition for tissue repair. However, a more pronounced scar was observed with the application of MPC. Table 5 summarizes cytokine expression in wounded control and diabetic skin, at day 3 and 10 post-wounding.

These results suggest that *in vivo* NT combined with the MPC foam application in diabetic wound dressings can promote an inflammatory response was able to reduce the inflammatory response, to promote an anti-inflammatory response and to stimulate re-

671 epithelialization which are important phases of the healing process. Human studies are
672 needed to further investigate the potential application of NT-loaded MPC wound
673 dressings as therapy for diabetic foot ulcers.
674
675 **Acknowledgments**
676 This work was financially supported by COMPETE , FEDER and Fundação para a
677 Ciência e Tecnologia (FCT-MEC) under contract PTDC/SAU-MII/098567/2008,
678 PTDC/SAU FAR/121109/2010 and PEst-C/EQB/UI0102/2011 and PEst-
679 C/SAU/LA0001/2013-2014, in addition to the EFSD/JDRF/Novo Nordisk European
680 Programme in Type 1 Diabetes Research and Sociedade Portuguesa de Diabetologia
681 (SPD).
682 Liane I. F. Moura, Ana M. A. Dias and Ermelindo Leal acknowledge FCT-MEC for
683 their fellowships SFRH/BD/60837/2009, SFRH/BPD/40409/2007 and
684 SFRH/BPD/46341/2008, respectively.
685
686 **Conflict of interest**
687 The authors declare no competing financial interest.
688
689 **Supplementary data**
690 Supplementary data associated with this article can be found, in the online version, at
691 doi: (to include later).
692
693 **References**
694
695 [1] Moura LI, Dias AM, Carvalho E, de Sousa HC. Recent advances on the
696 development of wound dressings for diabetic foot ulcer treatment-A review. Acta
697 biomaterialia 2013.
698 [2] Tellechea A, Leal E, Veves A, Carvalho E. Inflammatory and angiogenic
699 abnormalities in diabetic wound healing: role of neuropeptides and therapeutic
700 perspectives The Open Circulation and Vascular Journal 2010;3:43-55.
701 [3] Silva L, Carvalho E, Cruz MT. Role of neuropeptides in skin inflammation and its
702 involvement in diabetic wound healing. Expert Opin Biol Ther 2010;10:1427-39.
703 [4] Pradhan L, Nabzdyk C, Andersen ND, LoGerfo FW, Veves A. Inflammation and
704 neuropeptides: the connection in diabetic wound healing. Expert Rev Mol Med
705 2009;11:e2.
706 [5] Lazarus LH, Brown MR, Perrin MH. Distribution, localization and characteristics of
707 neurotensin binding sites in the rat brain. Neuropharmacology 1977;16:625-9.

[6] Sundler F, Hakanson R, Hammer RA, Alumets J, Carraway R, Leeman SE, et al. Immunohistochemical localization of neurotensin in endocrine cells of the gut. Cell and tissue research 1977;178:313-21.
[7] Brain SD. Sensory neuropeptides: their role in inflammation and wound healing. Immunopharmacology 1997;37:133-52.
[8] Kalafatakis K, Triantafyllou K. Contribution of neurotensin in the immune and neuroendocrine modulation of normal and abnormal enteric function. Regulatory peptides 2011;170:7-17.
[9] Scott JR, Tamura RN, Muangman P, Isik FF, Xie C, Gibran NS. Topical substance P increases inflammatory cell density in genetically diabetic murine wounds. Wound Repair and Regeneration 2008;16:529-33
[10] Pradhan L, Cai X, Wu S, Andersen ND, Martin M, Malek J, et al. Gene expression of pro-inflammatory cytokines and neuropeptides in diabetic wound healing. J Surg Res 2011;167:336-42.
[11] Sweitzer SM, Fann SA, Borg TK, Baynes JW, Yost MJ. What is the future of diabetic wound care? The Diabetes Educator 2006;32:197-210.
[12] Malafaya PB, Silva GA, Reis RL. Natural-origin polymers as carriers and scaffolds for biomolecules and cell delivery in tissue engineering applications. Adv Drug Deliv Rev 2007;59:207-33.
[13] Sell SA, Wolfe PS, Garg K, McCool JM, Rodriguez IA, Bowlin GL. The use of natural polymers in tissue engineering: a focus on electrospun extracellular matrix analogues. Polymers for Advanced Technologies 2010;2:522-53.
[14] Rinaudo M. Chitin and chitosan: properties and applications. Progress in Polymer Science 2006;31:603-32.
[15] Park CJ, Clark SG, Lichtensteiger CA, Jamison RD, Johnson AJW. Accelerated wound closure of pressure ulcers in aged mice by chitosan scaffolds with and without bFGF. Acta biomaterialia 2009;5:1926–36
[16] Huang S, Fu X. Naturally derived materials-based cell and drug delivery systems in skin regeneration. Journal of controlled release : official journal of the Controlled Release Society 2010;142:149-59.
[17] Dai T, Tanaka M, Huang YY, Hamblin MR. Chitosan preparations for wounds and burns: antimicrobial and wound-healing effects. Expert review of anti-infective therapy 2011;9:857-79.
[18] Takei T, Nakahara H, Ijima H, Kawakami K. Synthesis of a chitosan derivative soluble at neutral pH and gellable by freeze-thawing, and its application in wound care. Acta biomaterialia 2012;8:686-93.
[19] Berscht PC, Nies B, Liebendorfer A, Kreuter J. Incorporation of basic fibroblast growth factor into methylpyrrolidinone chitosan fleeces and determination of the in vitro release characteristics. Biomaterials 1994;15:593-600.
[20] Dai YN, Li P, Zhang JP, Wang AQ, Wei Q. A novel pH sensitive N-succinyl chitosan/alginate hydrogel bead for nifedipine delivery. Biopharmaceutics & drug disposition 2008;29:173-84.
[21] Tan Y, Han F, Ma S, Yu W. Carboxymethyl chitosan prevents formation of broad-spectrum biofilm. Carbohydr Polym 2011;84:1365-70.
[22] Chen X, Wang Z, Liu W, Park H. The effect of carboxymethyl-chitosan on proliferatyion and collagen secretion of normal and keloid skin fibroblasts. 2002;23:4609-14.
[23] Prabaharan M. Review Paper: Chitosan Derivatives as Promising Materials for Controlled Drug Delivery. J Biomater Appl 2008;23:5-38.

[24] Muzzarelli RAA, Ilari P, Tomasetti M. Preparation and characteristic properties of 5-methyl pyrrolidinone chitosan. Carbohydrate Polymers 1993;20:99-105.
[25] Santos KSCR, Silva HSRC, Ferreira EI, Bruns RE. 32Factorial design and response surfasse analysis optimization of N-carboxybutylchitosan synthesis. Carbohydrate Polymers 2005;59:37-42.
[26] Dias AMA, Rey-Ricob A, Oliveira RA, Marceneiro S, Alvarez-Lorenzo C, Concheiro A, et al. Wound dressings loaded with an anti-inflammatory jucá (Libidibia ferrea) extract using supercritical carbon dioxide technology. The Journal of Supercritical Fluids 2013;74:34-45.
[27] Brun P, Mastrotto C, Beggiao E, Stefani A, Barzon L, Sturniolo GC, et al. Neuropeptide neurotensin stimulates intestinal wound healing following chronic intestinal inflammation. Am J Physiol Gastrointest Liver Physiol 2005;288:G621-9.
[28] da Silva L, Neves BM, Moura L, Cruz MT, Carvalho E. Neurotensin downregulates the pro-inflammatory properties of skin dendritic cells and increases epidermal growth factor expression. Biochim Biophys Acta 2011;1813:1863-71.
[29] Obara K, Ishihara M, Fujita M, Kanatani Y, Hattori H, Matsui T, et al. Acceleration of wound healing in healing-impaired db/db mice with a photocrosslinkable chitosan hydrogel containing fibroblast growth factor-2. Wound repair and regeneration : official publication of the Wound Healing Society [and] the European Tissue Repair Society 2005;13:390-7.
[30] Rossi S, Marciello M, Sandri G, Ferrari F, Bonferoni MC, Papetti A, et al. Wound Dressings Based on Chitosans and Hyaluronic Acid for the Release of Chlorhexidine Diacetate in Skin Ulcer Therapy. Pharmaceutical Development and Technology 2007;12:415-22.
[31] Huang P, Han B, Liu W, Chang Q, Dong W. Preparation and Biocompatibility of N-carboxymethyl chitosan. Journal of Functional Materials 2009;7:25-33.
[32] Hwang SM, Chen CY, Chen SS, Chen JC. Chitinous materials inhibit nitric oxide production by activated RAW 264.7 macrophages. Biochemical and biophysical research communications 2000;271:229-33.
[33] Yang C, Zhou Y, Zhang X, Huang X, Wang M, Han Y, et al. A green fabrication approach of gelatin/CM-chitosan hybrid hydrogel for wound healing. Carbohydrate Polymers 2010;82:1297-305.
[34] Chen R, Wang G, Chen C, Ho H, Shen M. Development of a new N-O-(Carboxymethyl)/chitosan /collagen matrixes as a wound dressing. Biomacromolecules 2006;7:1058-64.
[35] Muzzarelli R. Depolymerization of methyl pyrrolidinone chitosan by lysozyme. Carbohydrate Polymers 1992;19:29-34.
[36] Enoch S, Leaper DJ. Basic Science of wound healing. Surgery 2008;26:31-7.
[37] Davidson JM. Animal models for wound repair. Archives of dermatological research 1998;290 Suppl:S1-11.
[38] Lehr C, Bouwstra JA, Schacht EH, Junginger HE. In vitro evaluation of mucoadhesive properties of chitosan and some other natural polymers. International Journal of Pharmaceutics 1992;78:43-8.
[39] Ono I, Tateshita T, Inoue M. Effect of a collagen matrix containing basic fibroblast growth factor on wound contraction. J Biomed Mater Res (Appl Biomater) 1999;48:621–30.
[40] Ishihara M, Ono K, Sato M, Nakanishi K, Saito Y, Yura H, et al. Acceleration of wound contraction and healing with a photocrosslinkable chitosan hydrogel. Wound

repair and regeneration : official publication of the Wound Healing Society [and] the European Tissue Repair Society 2001;9:513-21.
[41] Galkowska H, Wojewodzka U, Olszewski WL. Chemokines, cytokines, and growth factors in keratinocytes and dermal endothelial cells in the margin of chronic diabetic foot ulcers. Wound repair and regeneration : official publication of the Wound Healing Society [and] the European Tissue Repair Society 2006;14:558-65.
[42] Hansen SL, Myers CA, Charboneau A, Young DM, Boudreau N. HoxD3 accelerates wound healing in diabetic mice. The American journal of pathology 2003;163:2421-31.
[43] Bashir MM, Sharma MR, Werth VP. TNF-alpha production in the skin. Archives of dermatological research 2009;301:87-91.
[44] Lin Z, Kondo T, Ishida Y, Takayasu T, Mukaida N. Essential involvement of IL-6 in the skin wound-healing process as evidenced by delayed wound healing in IL-6 deficient mice. Journal of Leukocyte Biology 2003;73:713-21.
[45] Gabbiani G. The myofibroblast in wound healing and fibrocontractive diseases. The Journal of pathology 2003;200:500-3.
[46] Diegelmann RF, Evans MC. Wound healing: an overview of acute, fibrotic and delayed healing. Frontiers in bioscience : a journal and virtual library 2004;9:283-9.
[47] Singer AJ, Clark RA. Cutaneous wound healing. N Engl J Med 1999;341:738-46.
[48] Blakytny R, Jude EB. Altered molecular mechanisms of diabetic foot ulcers. Int J Low Extrem Wounds 2009;8:95-104.
[49] Crane NJ, Brown TS, Evans KN, Hawksworth JS, Hussey S, Tadaki DK, et al. Monitoring the healing of combat wounds using Raman spectroscopic mapping. Wound Repair Regen 2010;18:409-16.
[50] Verrecchia F, Mauviel A. TGF-beta and TNF-alpha: antagonistic cytokines controlling type I collagen gene expression. Cellular signalling 2004;16:873-80.
[51] Black E, Vibe-Petersen J, Jorgensen LN, Madsen SM, Agren MS, Holstein PE, et al. Decrease of collagen deposition in wound repair in type 1 diabetes independent of glycemic control. Arch Surg 2003;138:34-40.

Figures Captions

Figure 1. A) Chemical synthesis of chitosan derivatives: *N*-carboxymethyl chitosan (CMC), 5-methyl pyrrolidinone chitosan (MPC) and *N*-succinyl chitosan (SC). B) SEM micrographs for non-loaded chitosan derivatives CMC, MPC and SC representing the different structures obtained by freeze-drying. Inner images represent magnifications.

Figure 2. Water vapor (A) and water (B) swelling profiles observed for CMC (■), MPC (▲) and SC (♦) foams. The inserted figure represents a zoom of the water swelling profiles for the first monitored day. Lines serve only as guides for the eye. Results are presented as mean ± SEM of two independent experiments.

Figure 3. Release kinetic profiles for GSH from CMC (■), MPC (▲) and SC (♦) foams at pH 7 measured for 8 h at 37 ºC. Lines serve only as guides for the eye. Results are presented as mean ± SEM of two independent experiments.

Figure 4. Cell viability of Raw (A) and HaCaT (B) cells in the presence of CMC or MPC foams, during 24, 48 and 72 h. and NO production in Raw cells (C). Results are presented as mean ± SEM of three independent experiments.

Figure 5. Wound size measurements for MPC, NT and NT-loaded MPC foam treatments in either control (A) or diabetic (B) mice. The wound size was determined at days 0, 1, 3, 5, 8 and 10 post-wounding. Results are presented as mean ± SEM of seven to eighteen independent experiments. *$p < 0.05$ MPC compared to PBS, **$p < 0.01$ MPC compared to PBS, *** $p < 0.001$ MPC compared to PBS, # $p < 0.05$ MPC+NT compared to PBS, ## $p < 0.01$ MPC+NT compared to PBS, ### $p < 0.001$ MPC+NT compared to PBS, $ $p < 0.05$ NT compared to PBS, $$ $p < 0.01$ NT compared to PBS; §$p < 0.05$ NT compared to MPC+NT, §§ $p < 0.01$ NT compared to MPC+NT, && $p < 0.01$ MPC compared to MPC+NT.

Figure 6. The gene expression profile for TNF-α, IL-6, KC, IL-1β, COL1A1, COL1A2 and COL3A1 in skin biopsies before and after treatments, at either day 3 (A, C, E, G, I, K, M) or 10 (B, D, F, H, J, L, N) post wounding. Results are presented as mean ± SEM of seven to eighteen independent experiments. & $p < 0.05$ compared with PBS d3, *$p < 0.05$ compared with PBS d10, **$p < 0.01$ compared with PBS d10§ $p < 0.05$ compared with diabetic PBS d3, # $p < 0.05$ compared with diabetic PBS d10, # #$p < 0.01$ compared with diabetic PBS d10.

Figure 7. Protein expression of TNF-α and MMP-9 in unwounded skin (day 0) or after treatments, at either day 3 or 10 post-wounding. Results are presented as mean ± SEM of three to five independent experiments. & $p < 0.05$ compared with PBS d3, *$p < 0.05$ compared with PBS d10, **$p < 0.01$ compared with PBS d10§ $p < 0.05$ compared with diabetic PBS d3, # $p < 0.05$ compared with diabetic PBS d10, # #$p < 0.01$ compared with diabetic PBS d10.

Figure 8. Hydroxyproline content levels in unwounded skin (d0) or after treatments, at either day 3 or 10 post-wounding. Results are presented as mean ± SEM of four to six independent experiments. *p < 0.05 compared with PBS d10, § p < 0.05 compared with diabetic PBS d3, # #p < 0.01 compared with diabetic PBS d10.

Figure 9. Histopathological analysis of Hematoxicilin and Eosin (H&E) (Figure 9A) and Masson´s Trichrome (Figure 9B) staining for control and diabetic mouse skin, untreated or treated with MPC, NT and NT-loaded MPC foams (magnification 100×). Representative images of three skin stainings analyzed. a) Different repair process: in diabetic wounds, the granulation tissue is retained in dermis with overgoing fibroblast proliferation, at day 3 post-wounding (H&E;magnification 200×); b) Infiltrated PMN and lymphocytes in the granulation tissue in control mice, at day 3 post-wounding (H&E; magnification: 200×); c) Persistent inflammatory cells (neutrophils and lympho-plasmocitic cells) in PBS-treated diabetic mice, at day 10 post-wounding (H&E; magnification: 200×); d) Less inflammatory cells in granulation tissue when compared with c) in MPC-treated wounds, at day 10 post-wounding (H&E; magnification:200×); e) Less deposition of collagen in PBS-treated diabetic mice, at day 10 post-wounding (Masson´s Trichrome; magnification:200×); f) The granulation tissue is formed mainly by thin collagen fibers parallel to the epidermis (Masson´s Trichrome).

Supplementary data S1: ^{1}H-RMN spectra of chitosan, CMC, MPC and SC foams.

Supplementary data S2: Release kinetic profiles for GSH from CMC (■), MPC (▲) and SC (♦) foams at pH 6 (A) and 8 (B) measured for 8 h at 37 ºC. Lines serve only as guides for the eye. Results are presented as mean ± SEM of two independent experiments.

Supplementary data S3: The gene expression profile for MMP-9, EGF, VEGF ,PDGF, TGFβ1 and TGFβ3, in skin biopsies before and after treatments, at either day 3 (A, C, E, G, I, K) or 10 (B, D, F, H, J, L) post wounding. Results are presented as mean ± SEM of seven to eighteen independent experiments. & p < 0.05 compared with PBS d3, *p < 0.05 compared with PBS d10, **p < 0.01 compared with PBS d10§ p < 0.05

912 compared with diabetic PBS d3, # p < 0.05 compared with diabetic PBS d10, # #p <
913 0.01 compared with diabetic PBS d10.
914

List of tables

Table 1: Histological analysis of unwounded skin and NT, MPC and NT loaded MPC foams treated wounds at day 3, by H&E staining. - absence or no alterations, + presence <10%, ++ presence 10%,-50%, n.a, not applicable

	Skin control (d0)		**Day 3**							
			PBS		**MPC**		**NT**		**MPC+NT**	
	Control	Diabetic	Control	Diabetic	Control	Diabetic	Control	Diabetic	Control	Diabetic
New epidermis thickness										
- Stratus lucidum	-	+	-	+	+	++	-	+	+	++
- Epithelial layers	-	+	-	+	+	++	-	+	+	++
- Basal layer	-	+	-	+	+	++	-	+	+	++
Wound area (mm^2)	26.48 ±4.22	27.71±5.41	30.30±0.17	29.02±0.32	18.68±0.12	22.64±0.22	24.53±0.31	20.95±0.34	17.80±0.18	16.68±0.17
Re-epithelization										
- From bottom	na	na	+	-	+	-	+	-	+	-
- Top cover	na	na	-	+	-	+	-	+	-	+

Table 2: Histological analysis of NT, MPC and NT loaded MPC foams treated wounds at day 10, by H&E staining. - absence or no alterations, + presence <10%, ++ presence 10%,-50%, +++ presence >50%

	Day 10							
	PBS		**MPC**		**NT**		**MPC+NT**	
	Control	Diabetic	Control	Diabetic	Control	Diabetic	Control	Diabetic
New epidermis thickness								
- Stratus lucidum	++	+++	+	++	++	+++	+	++
- Epithelial layers	++	+++	+	++	++	+++	+	++
- Basal layer	++	+++	+	++	++	+++	+	++
Wound area (mm^2)	9.02±0.15	13.39±0.31	4.22±0.09	12.11±0.20	7.05±0.30	9.12±0.30	5.88±0.12	9.77±0.29
Re-epithelization								
- From bottom	+	-	+	-	+	-	+	-
- Top cover	-	+	-	+	-	+	-	+

Table 3: Inflammatory and granulation tissue histological analysis of NT, MPC and NT loaded MPC foams treated wounds at day 3, by H&E and Masson´s Trichrome staining. - absence or no alterations, + presence <10%, ++ presence 10%,-50%, +++ presence >50%; < not relevant, > predominant

	Day 3							
	PBS		MPC		NT		MPC+NT	
	Control	Diabetic	Control	Diabetic	Control	Diabetic	Control	Diabetic
Inflammation Status								
- PMN	++	+++	++	+	++	+	++	+
- Lymphocytes	+	++	+	-	+	-	+	-
- Plasma cells	-	-	-	-	-	-	-	-
- Fibrin	<	>	>	<	>	<	>	<
Repair								
- Fibroblasts	<	>	<	>	<	>	<	>
Collagen matrix								
- Loose	-	-	-	+	+	+	+	-
- Scar	-	-	-	+	-	+	+	++

Table 4: Inflammatory and granulation tissue histological analysis of NT, MPC and NT loaded MPC foams treated wounds at day 10, by H&E and Masson´s Trichrome staining. - absence or no alterations, + presence <10%, ++ presence 10%,-50%, +++ presence >50%;

	Day 10							
	PBS		MPC		NT		MPC+NT	
	Control	Diabetic	Control	Diabetic	Control	Diabetic	Control	Diabetic
Inflammation Status								
- PMN	-	++	-	+	-	+	-	+
- Lymphocytes	+	+++	+	++	+	++	+	++
- Plasma cells	+	+++	+	++	+	++	+	++
- Fibrin	-	-	-	-	-	-	-	-
Repair								
- Fibroblasts	++	+	+	++	+	+	+	+++
Collagen matrix								
- Loose	-	-	-	-	-	-	-	-
- Scar	++	+	+	++	+	+	+	+++

Table 5: Summary of cytokine and protein expression in wounded control and diabetic skin, at day 3 and 10 post-wounding.

Day	Cytokine/Growth factor	Control mice	Diabetic mice	Cell type that produce this protein
3	TNF-α	↓ MPC, NT, MPC+NT	↑ NT, MPC+NT	Macrophages, fibroblasts
	IL-6	↓ MPC; ↑ MPC+NT	↓ MPC, NT, MPC+NT	Macrophages, fibroblasts, Keratinocytes, endothelial cells
	KC	↑ MPC+NT	↓ MPC, NT, MPC+NT	Macrophages, fibroblasts
	IL-1β	↓ MPC, NT, MPC+NT	= MPC, NT, MPC+NT	Macrophages, epithelial cells
	COL1A1	=	↑ NT	Fibroblasts
	COL1A2	=	↑ NT	Fibroblasts
	COL3A1	↑ MPC+NT	↑ NT	Fibroblasts
10	TNF-α	↑ NT, MPC+NT	↓ NT, MPC+NT	Macrophages, fibroblasts
	IL-6	=	↓ MPC, NT, MPC+NT	Macrophages, fibroblasts, keratinocytes, endothelial cells
	KC	=	↓ MPC, NT, MPC+NT	Macrophages, fibroblasts
	IL-1β			Macrophages, epithelial cells
	COL1A1	↑NT,MPC+NT	↑MPC+NT	Fibroblasts
	COL1A2	↑NT,MPC+NT	↑MPC+NT	Fibroblasts
	COL3A1	↑NT	↑MPC+NT	Fibroblasts

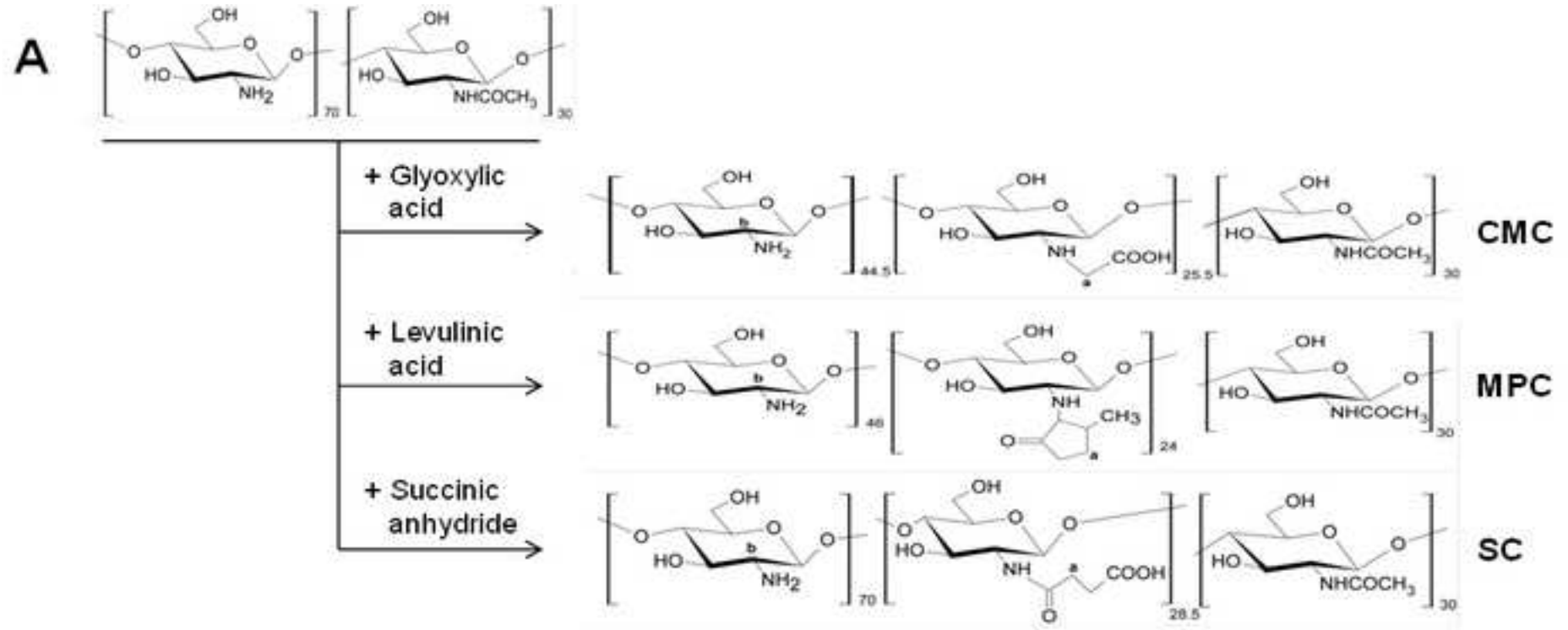

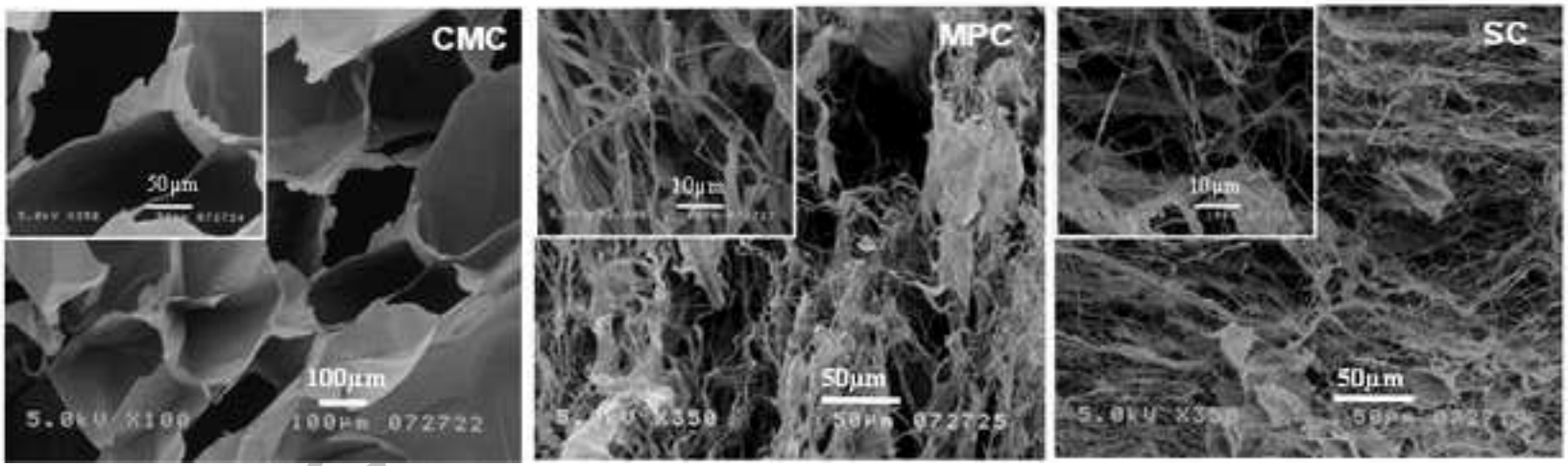

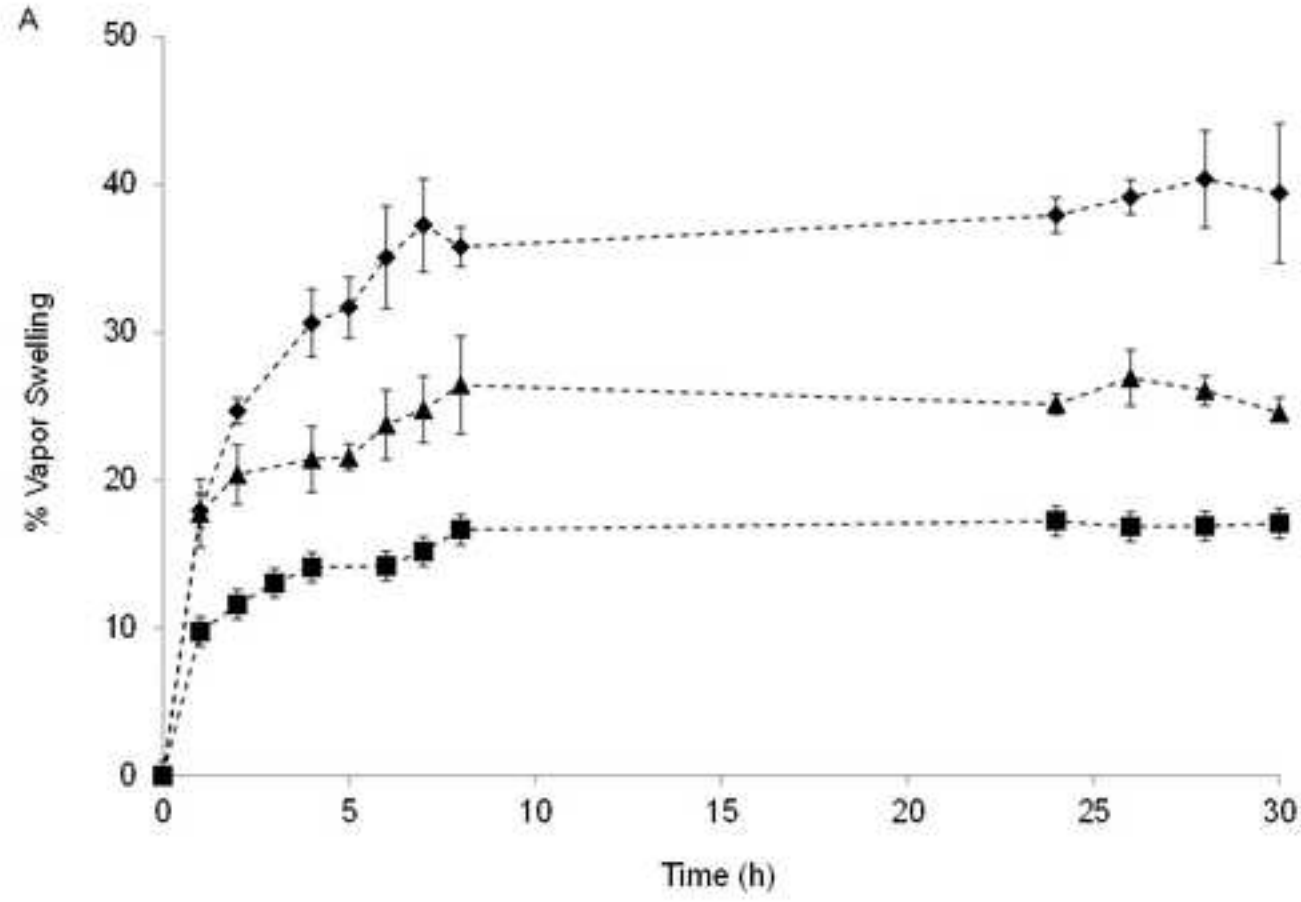

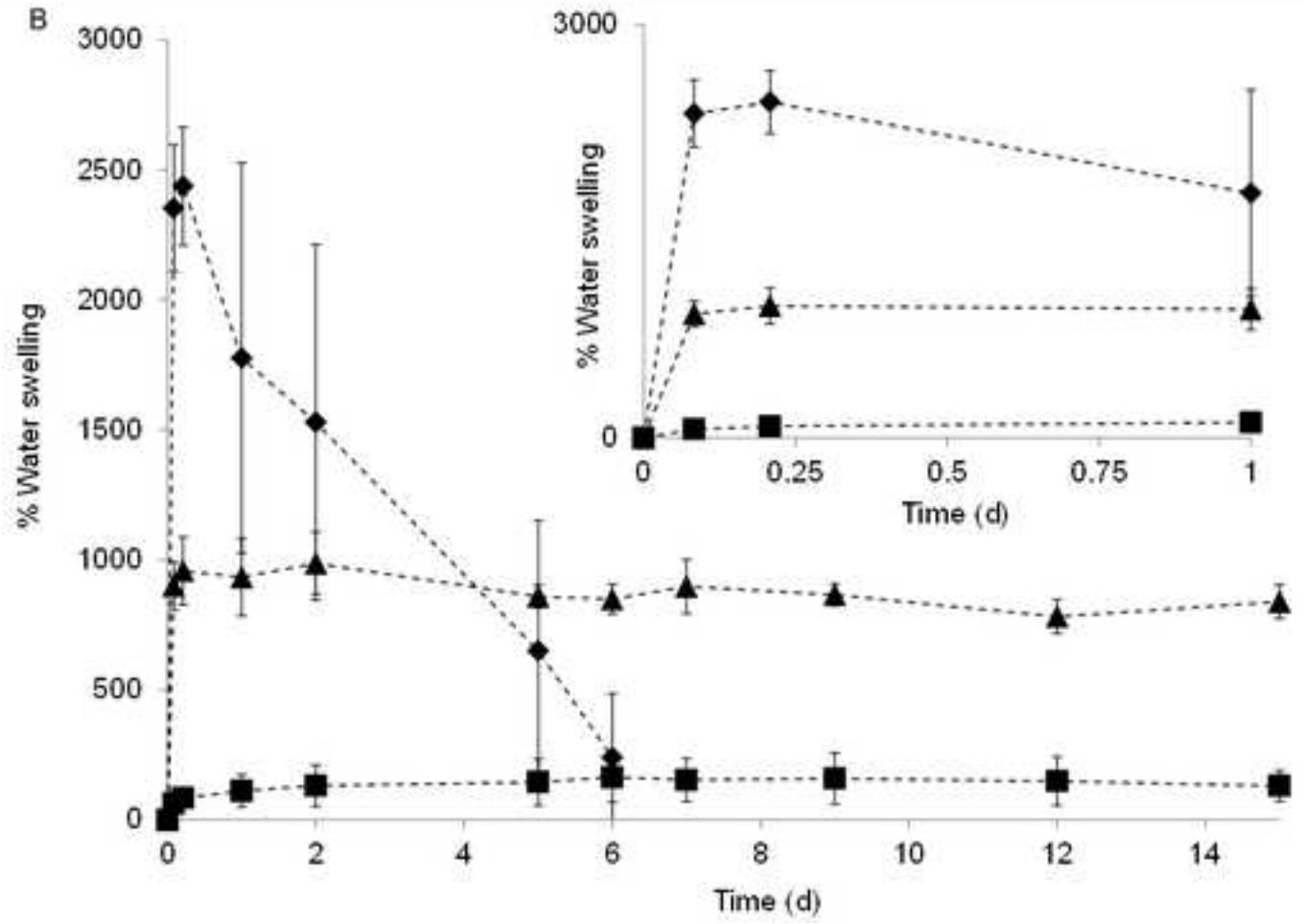

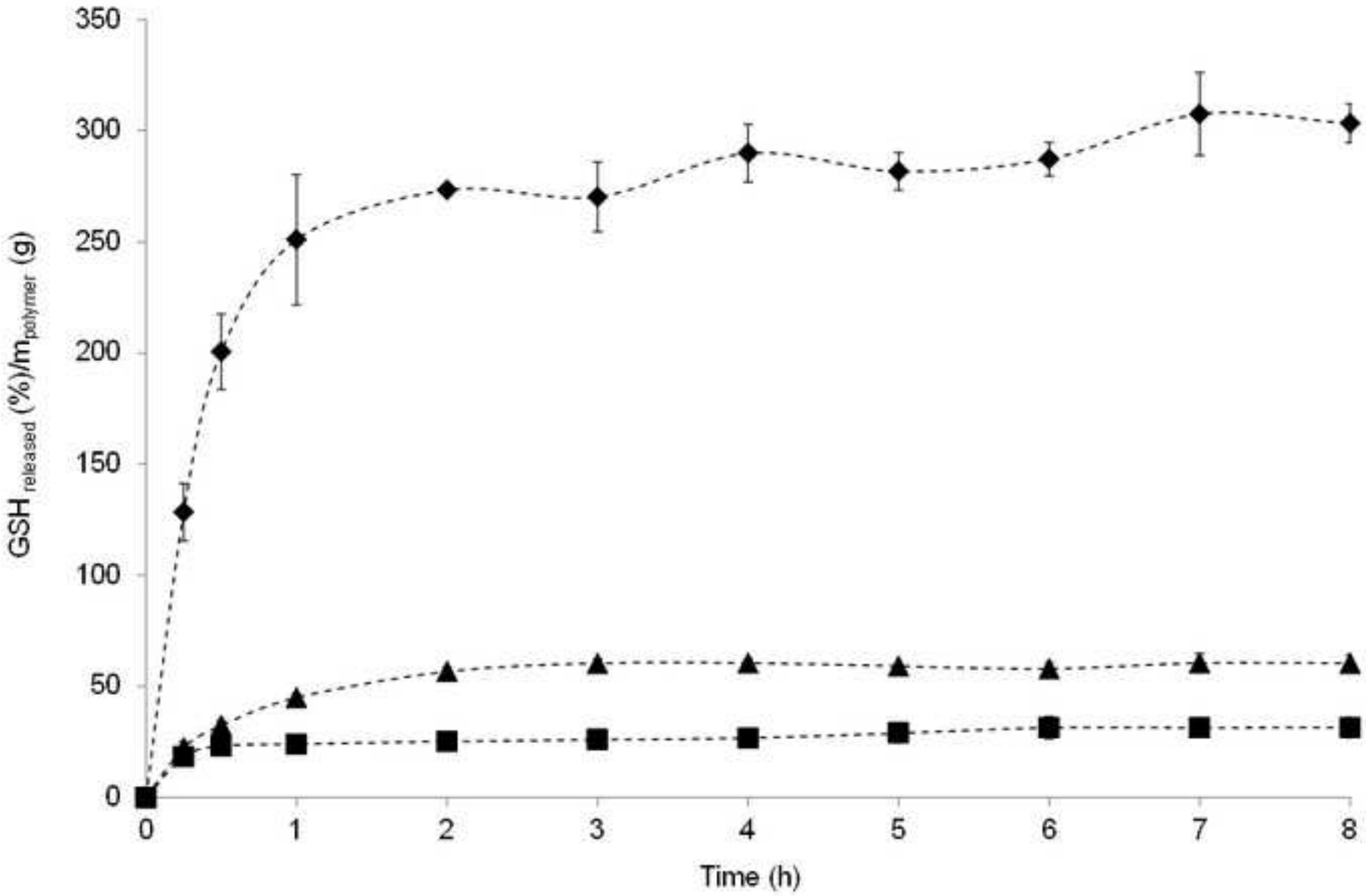

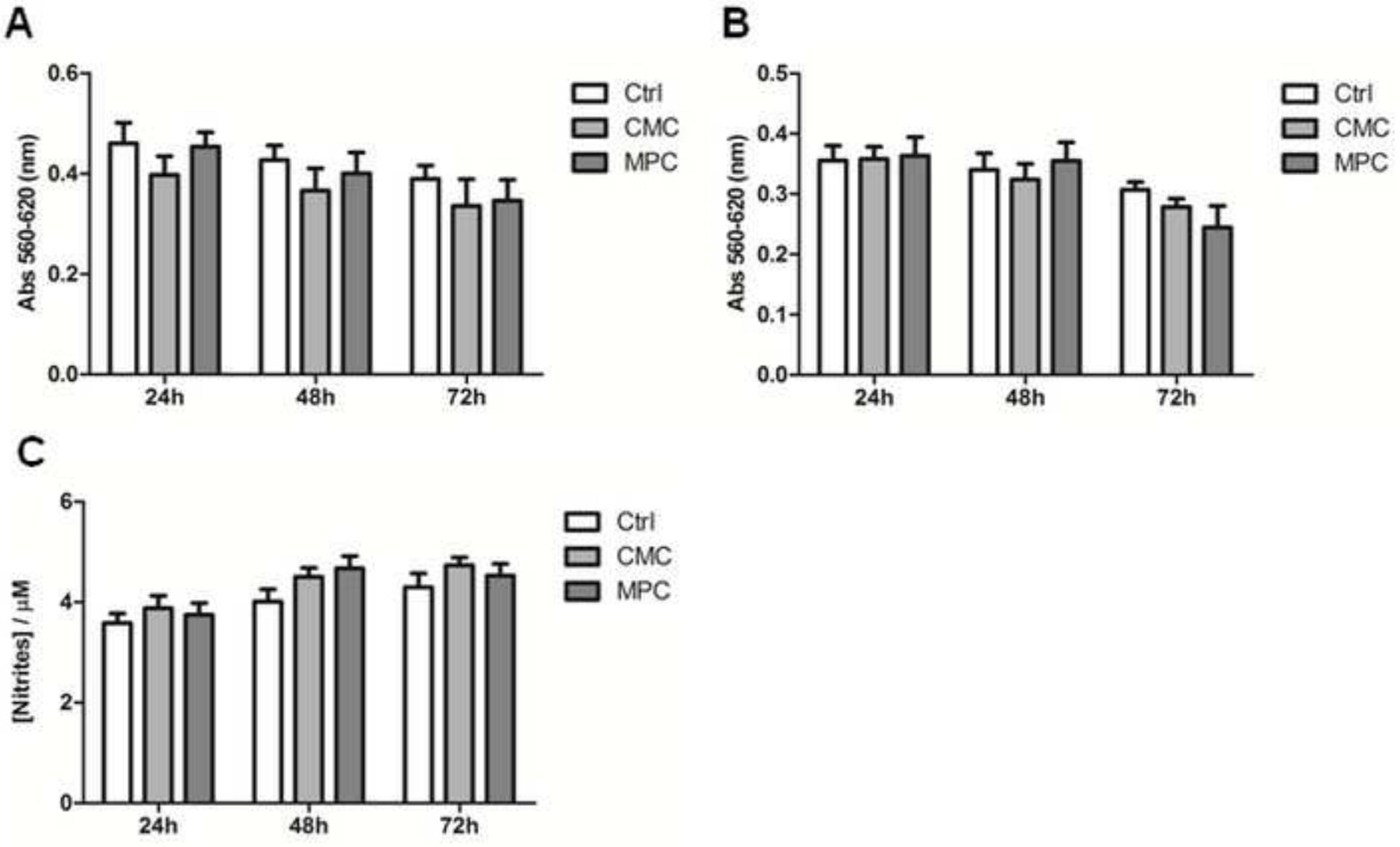

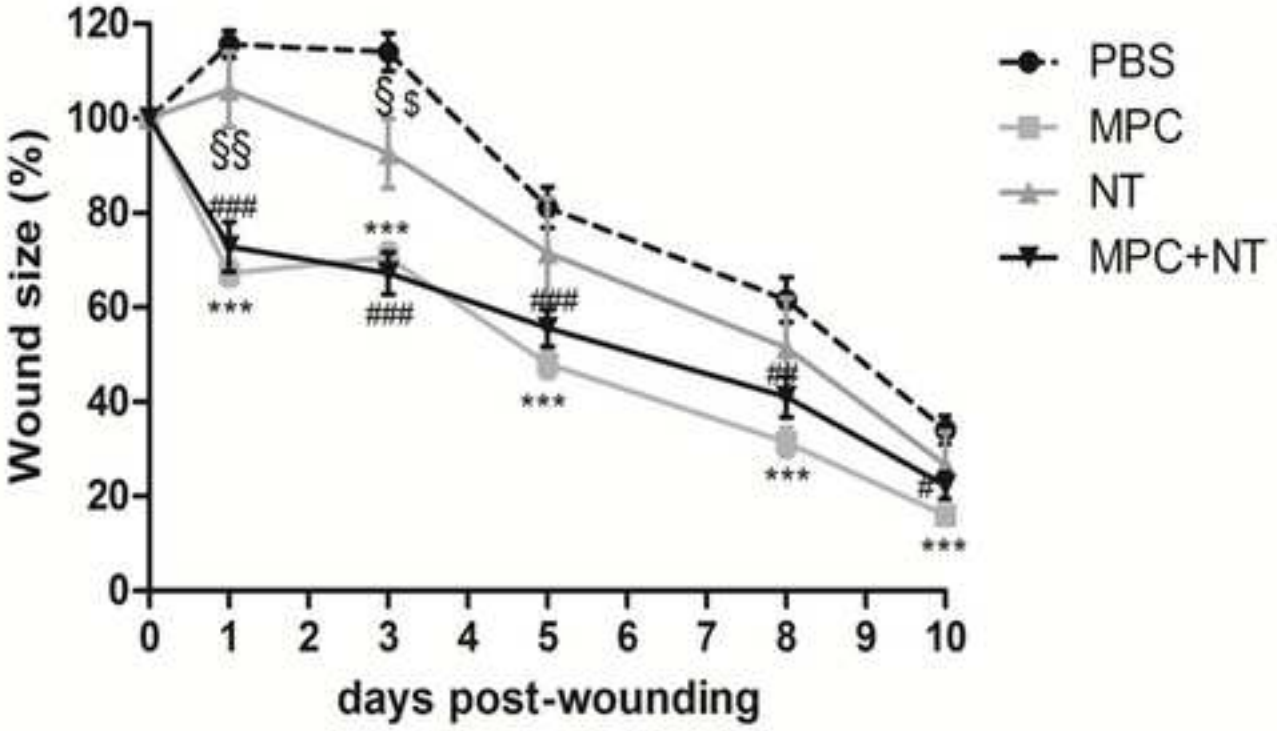
Wound size (%)
120
100
80
60
40
20
0
0 1 2 3 4 5 6 7 8 9 10
days post-wounding
PBS
MPC
NT
MPC+NT

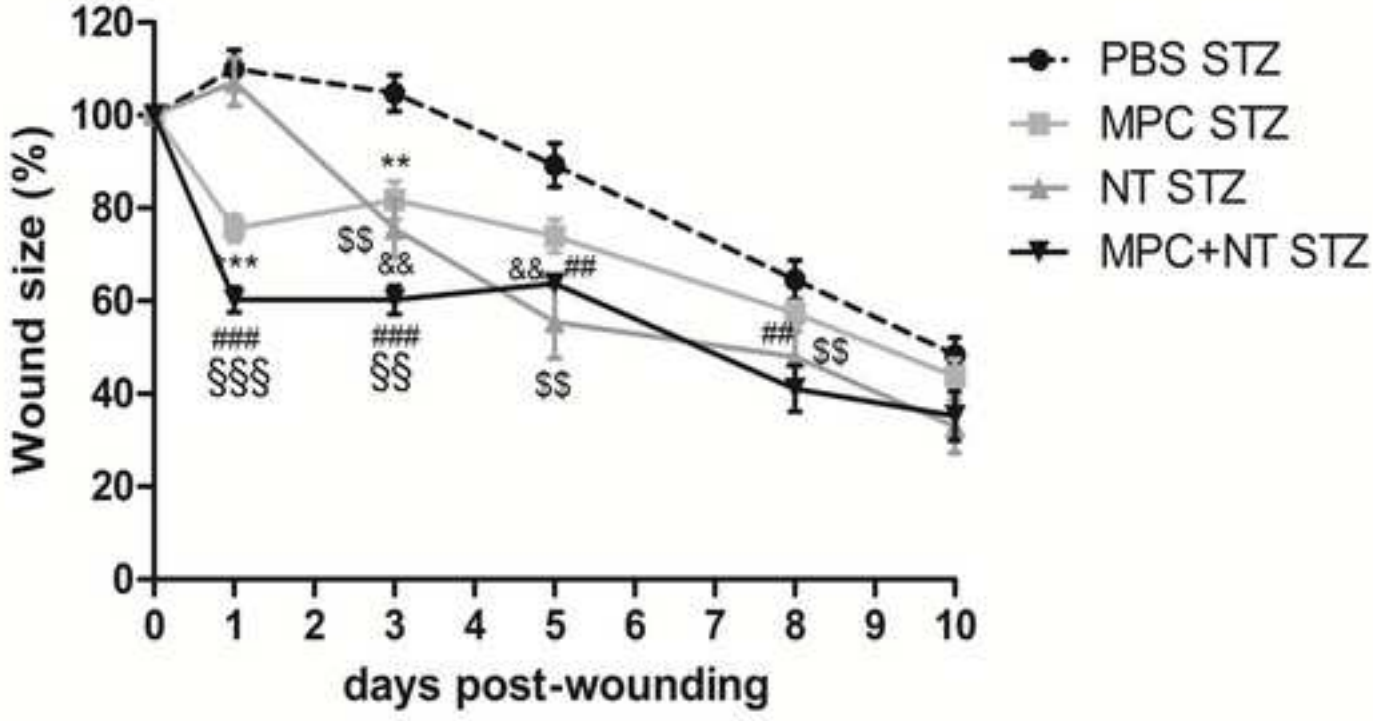
Wound size (%)
120
100
80
60
40
20
0
0 1 2 3 4 5 6 7 8 9 10
days post-wounding
PBS STZ
MPC STZ
NT STZ
MPC+NT STZ